

# Optically switchable transistor via energy-level phototuning in a bicomponent organic semiconductor

Emanuele Orgiu<sup>1</sup>, Núria Crivillers<sup>1</sup>, Martin Herder<sup>2</sup>, Lutz Grubert<sup>2</sup>, Michael Pätzel<sup>2</sup>, Johannes Frisch<sup>3</sup>, Egon Pavlica<sup>4</sup>, Duc T. Duong<sup>5</sup>, Gvido Bratina<sup>4</sup>, Alberto Salleo<sup>5</sup>, Norbert Koch<sup>3\*</sup>, Stefan Hecht<sup>2\*</sup> and Paolo Samorì<sup>1\*</sup>

**Organic semiconductors are suitable candidates for printable, flexible and large-area electronics. Alongside attaining an improved device performance, to confer a multifunctional nature to the employed materials is key for organic-based logic applications. Here we report on the engineering of an electronic structure in a semiconducting film by blending two molecular components, a photochromic diarylethene derivative and a poly(3-hexylthiophene) (P3HT) matrix, to attain phototunable and bistable energy levels for the P3HT's hole transport. As a proof-of-concept we exploited this blend as a semiconducting material in organic thin-film transistors. The device illumination at defined wavelengths enabled reversible tuning of the diarylethene's electronic states in the blend, which resulted in modulation of the output current. The device photoresponse was found to be in the microsecond range, and thus on a technologically relevant timescale. This modular blending approach allows for the convenient incorporation of various molecular components, which opens up perspectives on multifunctional devices and logic circuits.**

Soluble  $\pi$ -conjugated materials can be processed using methods that are suitable for the mass production of low-cost, flexible and light-weight 'plastic' electronics<sup>1,2</sup>, such as ink-jet printing and roll-to-roll methods, which opens up perspectives on the commercialization of organic electronic devices<sup>3-7</sup>. Great efforts have been devoted to the synthesis of new materials with tunable electronic properties, and to their electrical characterization<sup>8,9</sup>. A simple way to implement a multifunctional nature in a device relies on the use of different organic components that each confer a distinct property to the resulting hybrid material<sup>10-12</sup>. In the fabrication of organic thin-film transistors (OTFTs), blends of two or more electroactive components are used, typically by combining polymers and small molecules to best exploit the structural and electronic properties of both systems<sup>13</sup>. Among molecular switches as elements to integrate a multilevel logic in a material or device<sup>14</sup>, photochromic systems are attractive components that efficiently and reversibly interconvert between typically two (meta)stable isomers that exhibit remarkably different properties<sup>15</sup>. Therefore, such photochemically controlled bistable building blocks are able to translate an external optical stimulus into a change of the material's properties. Among the most promising candidates<sup>16</sup>, diarylethene (DAE)<sup>17</sup> photochromes offer the significant advantages of high fatigue resistance and thermal stability of both switching states, which (most importantly) are associated with radically different electronic properties, including energy levels that relate to the highest occupied molecular orbital (HOMO) and the lowest unoccupied molecular orbital and thus optical absorption and emission, as well as redox characteristics. These unique features were employed recently to modulate optically both charge-carrier

injection<sup>18</sup> and transport<sup>19</sup> in multilayer devices, such as photorewritable memories<sup>20</sup> and photoprogrammable organic light-emitting diodes<sup>21,22</sup>, by inserting an interfacial DAE layer. Furthermore, work on optical memories<sup>23</sup> and recent theoretical calculations<sup>24</sup> suggest that electrical current modulation can be obtained in blends of DAEs and organic semiconductors.

We fabricated bifunctional OTFTs by using blends of DAEs with an organic semiconducting polymer as the electroactive material. The dual functionality in our OTFTs was achieved by engineering the energy levels of the blend through the insertion of the DAE phototunable states in the polymer bulk to facilitate charge transport. Hence, blending the semiconducting material with a suitable DAE should enable the selective control and modulation of charge carriers within the film as a result of light illumination at different wavelengths, as predicted and shown in the two-terminal electrical characterization for spiropyran derivatives<sup>25</sup>.

## Results and discussion

We chose P3HT as one of the best-performing conjugated polymers for the semiconducting matrix because of its relatively high field-effect hole mobility in thin films<sup>26</sup> and easy processability in various organic solvents. Most importantly, its comparably low ionization energy (IE) makes it the ideal candidate for our study as it ensures an ohmic hole injection and/or extraction with gold electrodes<sup>27</sup>. Specifically, the IE of P3HT amounts to approximately 4.8 eV based on the oxidation potential measured by cyclic voltammetry (CV, see Supplementary Section 2.3) and the reported values from ultraviolet photoelectron spectroscopy (UPS) in thin films range from 4.4 eV to 4.9 eV (ref. 28). The varying IE values of

<sup>1</sup>Nanochemistry Laboratory, Institut de Science et d'Ingénierie Supramoléculaires, Unité Mixte de Recherche 7006, Centre National de la Recherche Scientifique, Université de Strasbourg, 8 allée Gaspard Monge, 67000 Strasbourg, France, <sup>2</sup>Department of Chemistry, Humboldt-Universität zu Berlin, Brook-Taylor-Straße 2, 12489 Berlin, Germany, <sup>3</sup>Institut für Physik, Humboldt-Universität zu Berlin, Newtonstraße 15, 12489 Berlin, Germany, <sup>4</sup>Laboratory for Organic Matter Physics, University of Nova Gorica, Vipavska 13, SI-5000 Nova Gorica, Slovenia, <sup>5</sup>Department of Materials Science and Engineering, Stanford University, Stanford, California 94305, USA. \*e-mail: samori@unistra.fr; norbert.koch@physik.hu-berlin.de; sh@chemie.hu-berlin.de

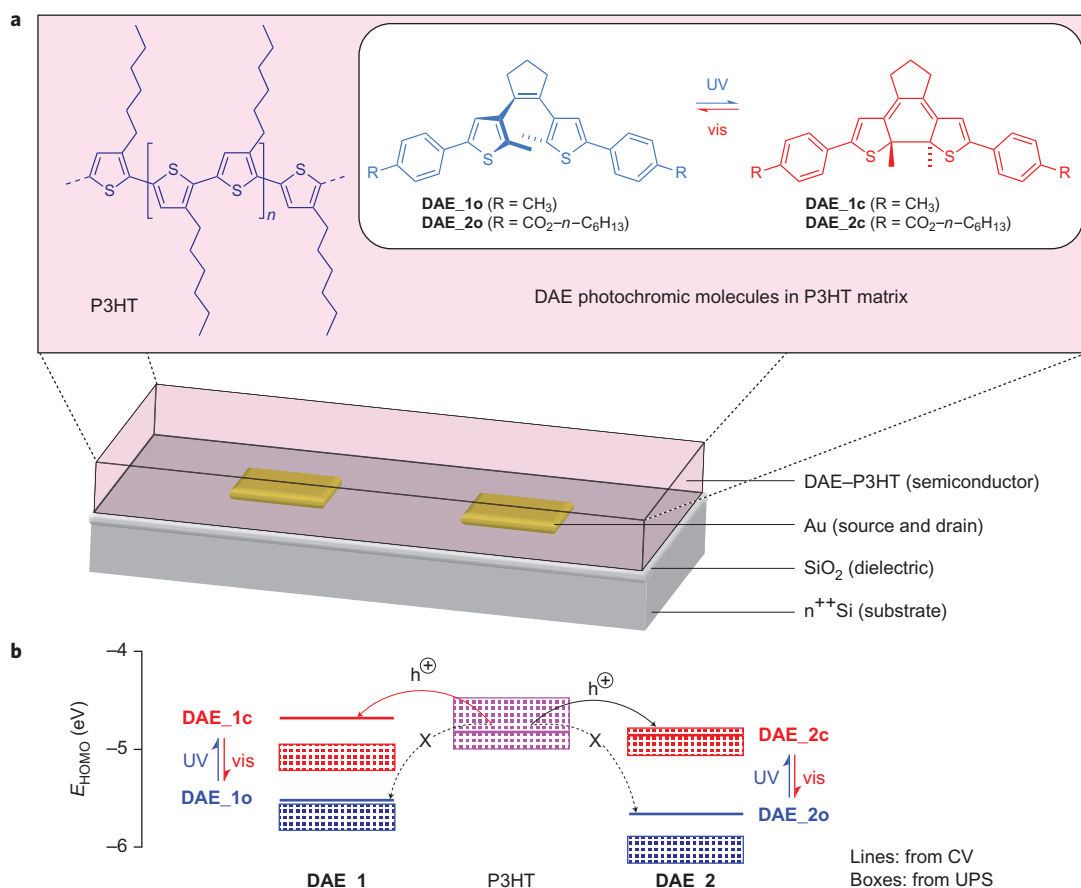


**Figure 1 | Devices components, geometry and energetics.** **a**, Schematic representation of the investigated OTFT devices, which includes chemical formulae of the molecular components, namely the photochromic molecules **DAE\_1** and **DAE\_2** in their two switching states, and of the P3HT semiconducting polymer. **b**, Energy level diagram that depicts the HOMO levels of the employed components and highlights the mechanism of photomodulation in the OTFT (for exact values from CV and UPS measurements see Supplementary Sections 2.3 and 2.4). UV = ultraviolet; vis = visible.

P3HT in the solid are due to the collective electrostatic effects of intramolecular polar bonds, which result in a dependence of the IE on the surface orientation of the molecules<sup>29</sup>.

Taking into account the hole transport levels of P3HT (which correspond, in good approximation, to the IEs determined by CV and UPS, respectively), we designed and synthesized a DAE molecule, **DAE\_1** (Fig. 1a), that featured different IEs of its open and closed isomer with respect to the IE of P3HT. To explore the role of different IEs in the two different DAE isomers with respect to the IE of P3HT we extended our study to **DAE\_2**, with higher IEs of both isomers. Indeed, according to CV measurements the IEs of **DAE\_1** and **DAE\_2** decreased significantly, by about 0.8 eV, on irradiation with ultraviolet light, which converted the ring-open isomers **DAE\_1o** and **DAE\_2o** into their respective ring-closed isomers **DAE\_1c** and **DAE\_2c** (Fig. 1b). Reversion of the switching process by white-light illumination yielded the respective ring-opened isomers with their original high IEs, which corresponded to a level below that of P3HT (from CV). To evidence the switching capacity and associated energy-level changes of the DAEs in their open and closed forms in solid films, UPS experiments were done exemplarily on thin films of **DAE\_1** and **DAE\_2** on indium tin oxide (ITO) substrates (see Supplementary Section 2.4). The IEs derived from UPS amounted to 5.1 eV and 5.2 eV for **DAE\_1c** and **DAE\_2c**, respectively. On illumination of such films with white light, the emission feature assigned to the HOMO of the closed forms disappeared and the spectrum became practically identical to those obtained for thin films made from the corresponding open forms, with **DAE\_1o** and **DAE\_2o** displaying IEs of 5.7 eV and

6.05 eV, respectively. Although the energy difference of the IEs between the open and closed isomers determined by CV in solution and by UPS in thin films are very similar, UPS fails to place the valence band maximum of P3HT (the polymer analogue to the molecular HOMO) between those of **DAE\_1o** and **DAE\_1c**, as obtained from CV. The reason is that IE values obtained via photoemission from the surface of individual material films are not always representative of the relative energy level positions within blended films because the electrostatic potentials generated by the intramolecular polar bonds mutually influence the relative placement of energy levels<sup>30</sup>. Consequently, the relative energy level positions in the P3HT/DAE blends investigated are probably better represented by the data obtained in solution from CV measurements.

To test the electrical properties of the blends, OTFT devices in bottom-contact bottom-gate geometry (Fig. 1a) were fabricated and characterized electrically. To prepare the devices, a solution of P3HT in chloroform containing the DAE was spun to form a thin film on a Si/SiO<sub>2</sub> substrate in-between the gold pre-patterned source and drain electrodes. For **DAE\_1o** the blend contained different concentrations relative to P3HT, from one to 40 wt%. Atomic force microscopy (AFM) studies (see Supplementary Section 2.5) revealed the absence of phase separation on a scale that ranged from 5 nm up to several tens of micrometres for all the considered blend ratios. Grazing incidence X-ray diffraction experiments at the Stanford Synchrotron Radiation Lightsource further revealed that neat films of **DAE\_1o**, **DAE\_1c** and **DAE\_2o** spin coated from chloroform were amorphous (see Supplementary Section 2.6). In addition, two-dimensional

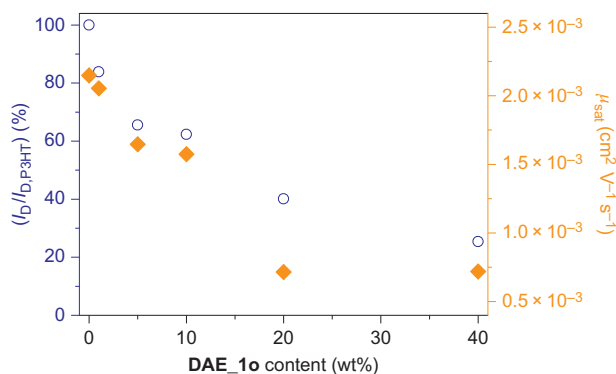


**Figure 2 | Photoresponse of current and mobility at different film compositions.** Drain current percentage (normalized to the drain current measured when using bare P3HT,  $I_{D,P3HT}$ ) versus **DAE\_1o** weight percentage in the blend. Almost a 75% decrease of the initial current value is achieved in the case of 40 wt% **DAE\_1o**. Each point (blue open circle) represents the drain current value taken at drain voltage  $V_D = -60$  V and gate voltage  $V_G = -80$  V on the output curves. On the right axis, the corresponding field-effect mobility variation (starting from the mobility of P3HT-based transistors) is shown (red diamonds).

diffraction patterns of P3HT films blended with DAE nearly matched those of neat P3HT films in terms of peak positions and widths. These data indicate that DAE molecules in both the open and closed forms do not disrupt significantly the molecular packing of P3HT, but prefer to reside within the amorphous domains of the semiconducting polymer. As charge transport in polythiophenes is believed to be dominated by propagation through interconnecting ordered regions<sup>31–33</sup>, this observation explains why the mobility of P3HT/DAE blended films remains relatively high, even on the introduction of up to 40% DAE (see below). Importantly, the photoswitching ability of the blend in the solid state was retained, as observed by ultraviolet–visible (UV/vis) spectroscopy on thin films (see Supplementary Section 2.2).

The blend-based OTFT devices show decreasing drain current ( $I_D$ ) with increasing amounts of **DAE\_1o** in the blend (Fig. 2), as **DAE\_1o** molecules act as scattering centres for positive charge carriers. As hole transport occurs predominantly via levels close to the P3HT valence-band maximum, the HOMO level of **DAE\_1o**, which has a higher binding energy by several 100 meV (see Fig. 1b), is not accessible for mobile holes. This energy-level situation was chosen to minimize the influence of **DAE\_1o** on charge transport in P3HT. Hence, even on the addition of 40 wt% **DAE\_1o**, the hole mobility decreased only by a factor of three (Fig. 2).

In an OTFT configuration, blends that contained 20 wt% of either **DAE\_1o** or **DAE\_2o** in P3HT were selected and employed as the electroactive layer to investigate the switching behaviour. A thorough electrical characterization, which included the output and transfer characteristics in the two isomers blended with P3HT, was carried out (see Supplementary Section 2.9). The highest current detected in the linear transfer characteristics during successive illuminations of the device with ultraviolet and visible light are reported in Fig. 3 for both **DAE\_1o** and **DAE\_2o**. The static photoswitching (for details see Supplementary Section 2.10) was found to be stable, reversible and reproducible over many illumination cycles and it features a markedly high current modulation on irradiation with both white and ultraviolet light (Fig. 3). The current responses are governed by the different HOMO levels of the two DAE derivatives in their respective switching states. However, on ultraviolet irradiation the largest drain current modulation (~80%) was observed for **DAE\_1c** (Fig. 3). This results from

the more favourable hole transfer from P3HT to the HOMO of **DAE\_1c** and thus hole trapping compared to that of **DAE\_2c**. Additional evidence for the switching process as the origin of current modulation arises from a reference OTFT device from a blend of P3HT with **DAE\_1c**, synthesized prior to device fabrication. In this case, the drain current increased on white-light illumination and  $I_D$  values are similar to those obtained with **DAE\_1o** (Supplementary Fig. S20). Reference OTFT devices made solely from P3HT showed a light-induced modulation of current of less than 10%, whereas the devices with P3HT/**DAE\_1o** blends exhibited a current modulation close to 80%. Furthermore, in the P3HT/DAE-based devices  $I_D$  decreased on ultraviolet irradiation, whereas it increased in P3HT-based OTFTs (Supplementary Fig. S21), in accordance with previous reports<sup>34</sup>.

Dynamic characterization of **DAE\_1o**/P3HT-based photo-switching transistors was performed by exposing the transistor to fast irradiation cycles (Fig. 4a) with the light source switched every five seconds between the two different wavelengths. This experiment revealed that the current in the device can be photomodulated reversibly on a timescale of seconds without showing fatigue for several irradiation cycles. In addition, the response time ( $t_r$ ) of the devices, that is the time between a laser pulse at a certain excitation wavelength and the instant at which a variation in current is measured before a decay takes place, was determined (see Supplementary Section 2.11). The devices showed  $t_r$  values of a few microseconds on irradiation with ultraviolet light ( $\lambda_{\text{irr}} = 313$  nm, blue line), as shown in Fig. 4b. After the laser light was pulsed over the whole channel of a **DAE\_1o**/P3HT-based transistor at  $t = 0$  (dashed vertical line), the induced variation of the drain current caused by the different illumination wavelengths was recorded.

Most importantly, the devices did not show any degradation of the photoswitchability, even after two months of storage under nitrogen (Supplementary Fig. S22).

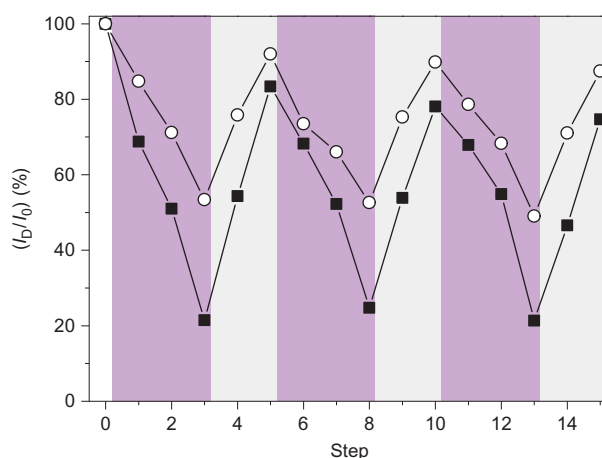


**Figure 3 | Reversible transistor characteristics.** Static photoswitching of the OTFT devices that contained **DAE\_1o** (20 wt% in P3HT, filled squares) or **DAE\_2o** (20 wt% in P3HT, open circles) at fixed time intervals (steps) of ultraviolet ( $\lambda_{\text{irr}} = 365$  nm, incident radiation power  $P_i = 62 \mu\text{W cm}^{-2}$ ) and white light ( $\lambda_{\text{irr}} > 400$  nm,  $P_i = 5.06 \text{ mW cm}^{-2}$ ) irradiation indicated by the violet and grey shaded areas, respectively. At the end of each step the light was turned off to measure a transfer curve. The values of the drain current taken from  $I_D$ - $V_G$  measurements at drain voltage  $V_D = -10$  V and gate voltage  $V_G = -80$  V are plotted (channel width  $W = 10,000 \mu\text{m}$ , channel length  $L = 20 \mu\text{m}$ ).  $I_0$  is the drain current, and normalizing factor  $I_0$  is the first drain-current value measured in step number 0 (in the dark) for each compound. The lines that connect the two series of points are used as guides to the eye. Details on the characterization procedure are provided in the Supplementary Information.

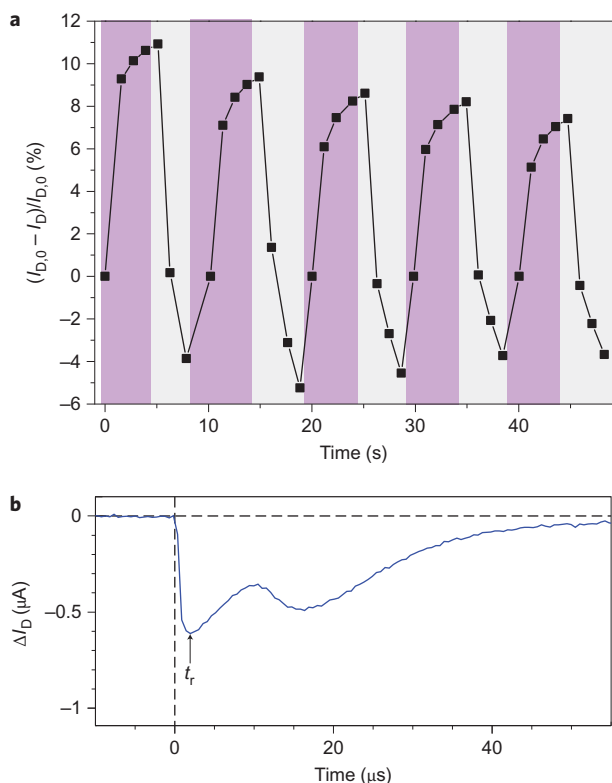


**Figure 4 | Time-resolved photoresponse.** **a**, Dynamic switching of an OTFT made from **DAE\_1o** (20 wt% in P3HT) under several irradiation cycles with ultraviolet ( $\lambda_{\text{irr}} = 365 \text{ nm}$ ,  $P_{\text{i}} = 62 \mu\text{W cm}^{-2}$ ) and white light ( $\lambda_{\text{irr}} > 400 \text{ nm}$ ,  $P_{\text{i}} = 5.06 \text{ mW cm}^{-2}$ ). The drain current,  $I_{\text{D}}$ , was recorded during irradiation and normalized to  $I_{\text{D},0}$ , which is the value that  $I_{\text{D}}$  assumes at the beginning of each cycle, which is every eight points. When the device was irradiated with ultraviolet light the negative drain current,  $I_{\text{D}}$ , decreased in the module with respect to the (negative) value that it assumed at the beginning of each cycle,  $I_{\text{D},0}$ . Hence, under ultraviolet irradiation the quantity  $(I_{\text{D},0} - I_{\text{D}})/I_{\text{D},0}$  becomes more and more positive in percentage with increasing the exposure time. On white-light illumination, the negative drain current,  $I_{\text{D}}$ , increases in the module and therefore makes the quantity  $(I_{\text{D},0} - I_{\text{D}})/I_{\text{D},0}$  decrease first and then become negative in percentage. This is consistent with an increase in drain current (in the module) when more and more **DAE\_1o** molecules switch from the closed state to the open state. During this experiment the transistor was polarized constantly at  $V_{\text{D}} = -10 \text{ V}$  and  $V_{\text{G}} = 0 \text{ V}$ . Before the measurement started, the device was allowed to stabilize (reaching saturation) in dark conditions. **b**, Drain current response of an OTFT made from **DAE\_1o** (20 wt% in P3HT) to a single laser pulse at 313 nm. Black arrows indicate the measured  $t_{\text{r}}$ . During the measurement the transistor was biased at  $V_{\text{D}} = -10 \text{ V}$  and  $V_{\text{G}} = -80 \text{ V}$ . Light was pulsed at 0 s, as indicated with a vertical dashed line. The laser pulse duration was 3 ns.

## Conclusion

In summary, we have demonstrated that the chemical and thus energetic tailoring of a bicomponent film can be exploited to confer multifunctional characteristics to a material. In particular, by blending a photochromic DAE derivative with P3HT, photochemically modulatable energetic levels were introduced into a semi-conducting thin film, and thereby offer a remote control of the output drain current in an OTFT by light stimuli at defined wavelengths. Chemical substitution of the DAEs allows for the modulation of the energy levels of each isomer, and thus renders possible their combination with a broad repertoire of molecular semiconducting systems to tailor the blend's properties. Our versatile approach renders unnecessary time-consuming and costly fabrication steps, such as the insertion of an additional

layer of photochromic molecules between semiconductor and dielectric<sup>22</sup>. Our strategy is fully compatible with ink-jet and roll-to-roll printing on large areas, which enables the design and fabrication of a new generation of organic phototransistors. As charge transport can be modulated by careful selection of the components in the blend, multifunctional devices that allow for multitasking with different wavelengths of light could readily be realized.

## Methods

For the synthesis and analysis of **DAE\_1** and **DAE\_2** see the Supplementary Information.

**Photochemistry in solution.** UV/vis spectroscopy was performed on a Cary 50 spectrophotometer equipped with a Peltier thermostatted cell holder at  $25 \pm 0.05 \text{ }^\circ\text{C}$  using spectrophotometric grade solvents. Irradiation experiments were carried out in  $\text{CH}_2\text{Cl}_2$  and  $\text{CH}_3\text{CN}$  in a quartz cuvette using an Oriel 68810 500 W mercury lamp in combination with an Oriel 77200 monochromator. Quantum yields were determined by comparing the initial reaction yields for the cyclization and the cycloreversion of the DAEs against the isomerization of azobenzene in methanol and the commercial furyl fulgide Aberchrome 670 in toluene, respectively.

**CV measurements.** These were performed using a PG310 USB (HEKA Elektronik) potentiostat interfaced to a PC with PotMaster v2x43 (HEKA Elektronik) software for data evaluation. The three-electrode configuration used was contained in a non-divided cell that consisted of a platinum disc (of diameter 1 mm) as working electrode, a platinum plate as counterelectrode and a saturated calomel electrode with an agar-agar plug in a Luggin capillary with a diaphragm as reference electrode. Measurements were carried out in acetonitrile (high-performance liquid chromatography grade) or dichloromethane (dried over calcium hydride and distilled) that contained 0.1 M  $\text{Bu}_4\text{NPF}_6$  using a scan rate of  $dE/dt = 1 \text{ V s}^{-1}$ . The data are given in reference to the ferrocene redox couple ( $\text{Fc}/\text{Fc}^+$ ), which was used as the external standard.

**UPS experiments.** A custom-made multichamber ultrahigh vacuum system at Humboldt-Universität zu Berlin was used. Photoelectrons were excited with 21.2 eV photons (He-discharge lamp) at a very low excitation density (about 100 times attenuated compared to those of standard commercial sources) and measured with a hemispherical spectrometer (SPECS Phoibos 100). The secondary electron cutoff spectra were recorded with samples biased at  $-10 \text{ V}$  to clear the analyser work function. Samples for UPS were prepared by spin-coating solutions, each of open and closed isomers, respectively, onto solvent-cleaned coons of ITO-coated glass in an inert gas box. Sample transfer to a ultrahigh vacuum proceeded within five minutes to reduce possible contamination from the air. During sample preparation, transfer and measurements, the samples were either kept in the dark or limited to irradiation with low-intensity red light. Switching of films from the closed to the open form was achieved with white-light illumination (halogen lamp) through a vacuum glass port and was completed within about ten minutes.

**AFM characterization.** A Veeco Dimension 3100 AFM running with a Nanoscope IV controller was used. AFM images were recorded in the intermittent contact (tapping) mode under ambient conditions. Standard silicon cantilevers were used (Veeco MPP-11100) with a nominal spring constant of  $40 \text{ N m}^{-1}$ , resonance frequency of 300 kHz and tip radius of 10 nm.

**OTFT preparation.**  $n^{++}$  Si/ $\text{SiO}_2$  substrates were exposed to pre-patterned interdigitated gold source and drain electrodes (IPMS Fraunhofer). After accurate cleaning of the substrates, a  $1 \text{ mg ml}^{-1}$  solution of P3HT (BASF Chemicals) was spin cast onto the substrates. Electrical characterization was performed in an inert environment (glovebox, with water and oxygen levels lower than 2 ppm) by means of an electrometer, Keithley 2636A, interfaced by LabTracer<sup>TM</sup> software.

**Characterization of the time responses of DAE\_1o(20%)/P3HT-based transistors through pulsed laser light at different wavelengths.** The measurements were performed by a 3 ns pulse tunable wavelength laser Ekspla NT342. The samples were illuminated with a monochromatic light ( $\lambda_{\text{irr}} = 313 \text{ nm}$ ) in the direction normal to the surface. Consequently, the whole channel was exposed to the light. The measurements were performed in the dark and under a controlled  $\text{N}_2$  atmosphere with the  $\text{O}_2$  level below 5 ppm and the water vapour level below 3 ppm. The response of the transistor to the light pulses was monitored as a time dependence of the drain current  $I_{\text{D}}(t)$ .

Received 27 February 2012; accepted 18 May 2012; published online 24 June 2012

## References

1. Arias, A. C., MacKenzie, J. D., McCulloch, I., Rivnay, J. & Salleo, A. Materials and applications for large area electronics: solution-based approaches. *Chem. Rev.* **110**, 3–24 (2010).

- Klauk, H., Zschieschang, U., Pflaum, J. & Halik, M. Ultralow-power organic complementary circuits. *Nature* **445**, 745–748 (2007).
- Crone, B. *et al.* Large-scale complementary integrated circuits based on organic transistors. *Nature* **403**, 521–523 (2000).
- Noh, Y. Y., Zhao, N., Caironi, M. & Sirringhaus, H. Downscaling of self-aligned, all-printed polymer thin-film transistors. *Nature Nanotech.* **2**, 784–789 (2007).
- Smits, E. C. P. *et al.* Bottom-up organic integrated circuits. *Nature* **455**, 956–959 (2008).
- Yan, H. *et al.* A high-mobility electron-transporting polymer for printed transistors. *Nature* **457**, 679–U671 (2009).
- Sekitani, T. *et al.* Stretchable active-matrix organic light-emitting diode display using printable elastic conductors. *Nature Mater.* **8**, 494–499 (2009).
- McCulloch, I. *et al.* Liquid-crystalline semiconducting polymers with high charge-carrier mobility. *Nature Mater.* **5**, 328–333 (2006).
- Gundlach, D. J. *et al.* Contact-induced crystallinity for high-performance soluble acene-based transistors and circuits. *Nature Mater.* **7**, 216–221 (2008).
- Berggren, M. *et al.* Light-emitting diodes with variable colors from polymer blends. *Nature* **372**, 444–446 (1994).
- Halls, J. J. M. *et al.* Efficient photodiodes from interpenetrating polymer networks. *Nature* **376**, 498–500 (1995).
- Yu, G., Gao, J., Hummelen, J. C., Wudl, F. & Heeger, A. J. Polymer photovoltaic cells: enhanced efficiencies via a network of internal donor–acceptor heterojunctions. *Science* **270**, 1789–1791 (1995).
- Smith, J. *et al.* The influence of film morphology in high-mobility small-molecule:polymer blend organic transistors. *Adv. Funct. Mater.* **20**, 2330–2337 (2010).
- Collier, C. P. *et al.* Electronically configurable molecular-based logic gates. *Science* **285**, 391–394 (1999).
- Russew, M. M. & Hecht, S. Photoswitches: from molecules to materials. *Adv. Mater.* **22**, 3348–3360 (2010).
- Tsuyoshi, T. & Irie, M. Electrical functions of photochromic molecules. *J. Photochem. Photobiol. C: Photochem. Rev.* **11**, 1–14 (2010).
- Irie, M. Diarylethenes for memories and switches. *Chem. Rev.* **100**, 1685–1716 (2000).
- Kronemeijer, A. J. *et al.* Reversible conductance switching in molecular devices. *Adv. Mater.* **20**, 1467–1473 (2008).
- Tsujioaka, T. & Masuda, K. Electrical carrier-injection and transport characteristics of photochromic diarylethene films. *Appl. Phys. Lett.* **83**, 4978–4980 (2003).
- Yoshida, M. *et al.* Development of field-effect transistor-type photorewritable memory using photochromic interface layer. *Jpn J. Appl. Phys.* **49**, 04DK09–04DK09–4 (2010).
- Zhang, Z. *et al.* A smart light-controlled carrier switch in an organic light emitting device. *Adv. Funct. Mater.* **18**, 302–307 (2008).
- Zacharias, P., Gather, M. C., Kohnen, A., Rehmann, N. & Meerholz, K. Photoprogrammable organic light-emitting diodes. *Angew. Chem. Int. Ed.* **48**, 4038–4041 (2009).
- Koshido, T., Kawai, T. & Yoshino, K. Novel photomemory effects in photochromic dye-doped conducting polymer and amorphous photochromic dye layer. *Synthetic Met.* **73**, 257–260 (1995).
- Jakobsson, F. L. E. *et al.* Tuning the energy levels of photochromic diarylethene compounds for opto-electronic switch devices. *J. Phys. Chem. C* **113**, 18396–18405 (2009).
- Andersson, P., Robinson, N. D. & Berggren, M. Switchable charge traps in polymer diodes. *Adv. Mater.* **17**, 1798–1803 (2005).
- Sirringhaus, H. *et al.* Two-dimensional charge transport in self-organized, high-mobility conjugated polymers. *Nature* **401**, 685–688 (1999).
- Burgi, L., Richards, T. J., Friend, R. H. & Sirringhaus, H. Close look at charge carrier injection in polymer field-effect transistors. *J. Appl. Phys.* **94**, 6129–6137 (2003).
- Zhang, F. *et al.* Energy level alignment and morphology of interfaces between molecular and polymeric organic semiconductors. *Org. Electron.* **8**, 606–614 (2007).
- Duhm, S. *et al.* Orientation-dependent ionization energies and interface dipoles in ordered molecular assemblies. *Nature Mater.* **7**, 326–332 (2008).
- Salzmann, I. *et al.* Tuning the ionization energy of organic semiconductor films: the role of intramolecular polar bonds. *J. Am. Chem. Soc.* **130**, 12870 (2008).
- Yang, H. *et al.* Effect of mesoscale crystalline structure on the field-effect mobility of regioregular poly(3-hexyl thiophene) in thin-film transistors. *Adv. Funct. Mater.* **15**, 671 (2005).
- Brinkmann, M. & Rannou, P. Molecular weight dependence of chain packing and semicrystalline structure in oriented films of regioregular poly(3-hexylthiophene) revealed by high-resolution transmission electron microscopy. *Macromolecules* **42**, 1125 (2009).
- Joshi, S. *et al.* Bimodal temperature behavior of structure and mobility in high molecular weight P3HT thin films. *Macromolecules* **42**, 4651–4660 (2009).
- Scarpa, G., Martin, E., Locci, S., Fabel, B. & Lugli, P. Organic thin-film phototransistors based on poly(3-hexylthiophene). *J. Phys. Conf. Ser.* **193**, 012114 (2009).

### Acknowledgements

This paper is dedicated to Professor Klaus Müllen on the occasion of his 65th birthday. This work was financially supported by European Community's Marie-Curie Initial Training Networks SUPERIOR (PITN-GA-2009-238177) and GENIUS (PITN-GA-2010-264694), Seventh Framework Programme FP7 ONE-P large-scale project no. 212311, European Research Council project SUPRAFUNCTION (GA-257305) and the International Center for Frontier Research in Chemistry. Generous support by the German Research Foundation (DFG via SFB 658 subproject B8 and via SPP 1355) is acknowledged. Access to UPS was granted by J.P. Rabe (Humboldt-Universität zu Berlin). BASF AG, Bayer Industry Services and Sasol Germany are thanked for generous donations of chemicals. A.S. acknowledges financial support from the National Science Foundation in the form of a CAREER Award. D.T.D. is supported by a Stanford Graduate Fellowship and the National Science Foundation Graduate Research Fellowship. Portions of this research were carried out at the Stanford Synchrotron Radiation Lightsource, a national user facility operated by Stanford University on behalf of the Office of Basic Energy Sciences, US Department of Energy.

### Author contributions

S.H. and P.S. conceived the experiments and designed the study. M.H., M.P. and L.G. carried out the synthesis as well as photochemical and electrochemical characterization. E.O. and N.C. performed the device experiments. E.O., G.B. and E.P. designed and performed the time-response measurements. J.F. carried out the UPS measurements. D.T.D. and A.S. performed the grazing incidence X-ray diffraction experiments. All authors discussed results and contributed to the interpretation of data. E.O., P.S., N.K. and S.H. co-wrote the paper. All authors contributed to editing the manuscript.

### Additional information

The authors declare no competing financial interests. Supplementary information accompanies this paper at [www.nature.com/naturechemistry](http://www.nature.com/naturechemistry). Reprints and permission information is available online at <http://www.nature.com/reprints>. Correspondence and requests for materials should be addressed to P.S., N.K., and S.H.